We are IntechOpen, the world's leading publisher of Open Access books Built by scientists, for scientists

4,800
Open access books available

122,000
International authors and editors

135M
Downloads

Our authors are among the

154
Countries delivered to

TOP 1%
most cited scientists

12.2%
Contributors from top 500 universities

CLARIVATE ANALYTICS
BOOK CITATION INDEX
INDEXED

WEB OF SCIENCE™

Selection of our books indexed in the Book Citation Index
in Web of Science™ Core Collection (BKCI)

Interested in publishing with us?
Contact book.department@intechopen.com

Modeling, Simulation, and Control of Steam Generation Processes

Graciano Dieck-Assad, José Luis Vega-Fonseca,
Isaías Hernández-Ramírez and
Antonio Favela-Contreras

Additional information is available at the end of the chapter

Abstract

This chapter describes a modeling methodology to provide the main characteristics of a simulation tool to analyze the steady state, transient operation, and control of steam generation processes, such as heat recovery steam generators (HRSG). The methodology includes a modular strategy that considers individual heat exchangers such as: economizers, evaporators, superheaters, drum tanks, and control systems. The modular strategy consists of the development of a numerical modeling tool that integrates sub-models based upon first principle equations of mass, energy, and momentum balance. The main heat transfer mechanisms characterize the dynamics of steam generation systems during normal and abnormal operations, which include the response of key process variables such as vapor pressure, temperature, and mass flow rate. Other important variables are: gas temperature, fluid temperature, drum pressure, drum's liquid level, and mass flow rate at each module. Those variables are usually analyzed with design predicted performance of real industrial equipment such as HRSG systems. Finally, two case studies of the application of the modeling strategy are provided to show the effectiveness and utility of the methodology.

Keywords: steam generation, modeling methodology, first principle equations, heat recovery steam generators (HRSG), boiler modeling, economizer, superheater, heat exchange surfaces, heat exchanger

1. Introduction

Electric energy production and conservation has become a key technological challenge in the development of nations to promote their steady and healthy socioeconomic development. Also,

the new technological developments to support Industry 4.0 and Internet of Things (IoT) require the solution of medium scale system models to optimize the performance of energy sources remotely by the incorporation of site-specific performance indices Ref [1–6]. Nowadays, the most common electric energy production process uses heat exchangers to transfer their calorific energy from flue gases to water-vapor that impinge prime movers connected to electric generators. The gas turbine is one of the best option in quick load following combined cycle power units due to their low costs in initial investment, operation, low emissions, and low reaction time or response time in generating electric energy from scratch. In this case, two-third of the mechanical work is used to self-power the operation of the turbine system and the rest can be used to generate electric energy. This characteristic produces an estimated efficiency between 25 and 45% [1] in gas turbine systems. Thermal and energetic engineering has developed methods to increase the efficiency in energy generation processes such that residues of a particular process can be used to drive another heat exchange process, and therefore, this technique is called cogeneration. The most common cogeneration technique takes advantage of the residual heat of a gas turbine to produce useful thermal energy loaded to vapor or heated air, and then, this energy is used in other industrial processes to increase electric energy production.

An example of vapor production uses a heat recovery steam generator (HRSG). **Figure 1** shows a HRSG and its components, where the inlet illustrates the hot gases coming from the gas turbine. The hot or flue gases transfer heat to different tube banks driving water as the working fluid and its pressure and temperature increase until reaching the required operating predicted performance conditions. This chapter discusses a methodology to develop and simulate models of steam generation processes in steady state and transient conditions from the stand point of thermos-hydraulics. The methodology can produce good simulation tools to evaluate system operation in startup, shutdown, stand by, and load changes during useful
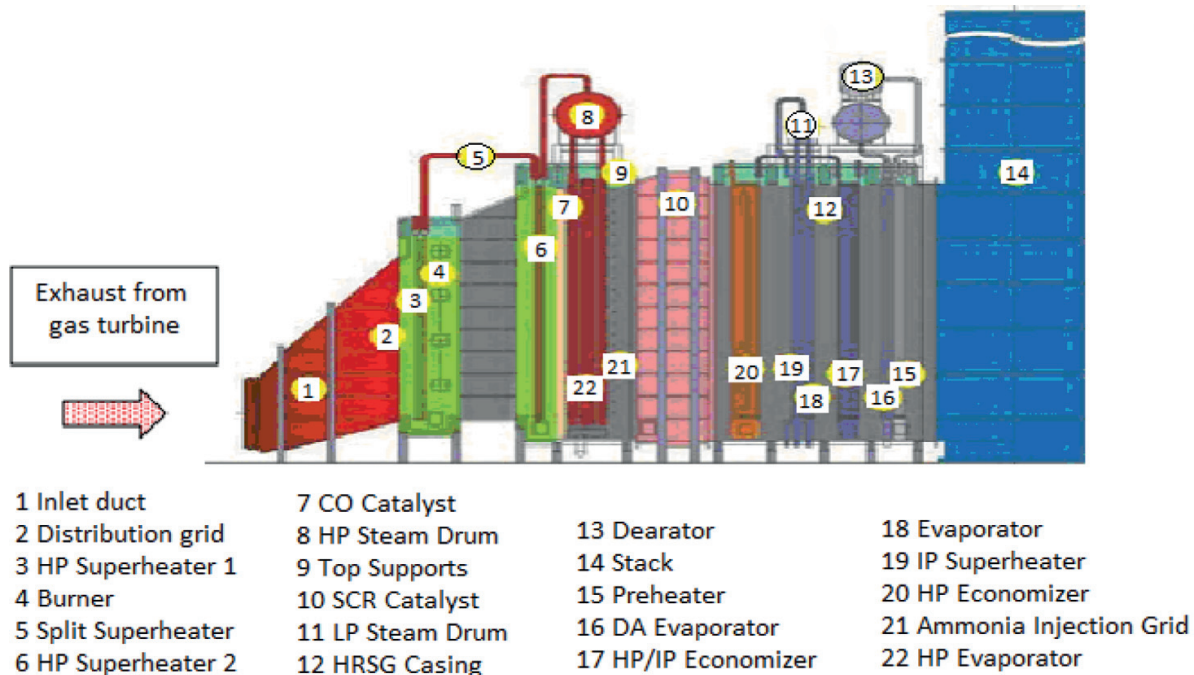

1 Inlet duct	7 CO Catalyst	13 Dearator	18 Evaporator
2 Distribution grid	8 HP Steam Drum	14 Stack	19 IP Superheater
3 HP Superheater 1	9 Top Supports	15 Preheater	20 HP Economizer
4 Burner	10 SCR Catalyst	16 DA Evaporator	21 Ammonia Injection Grid
5 Split Superheater	11 LP Steam Drum	17 HP/IP Economizer	22 HP Evaporator
6 HP Superheater 2	12 HRSG Casing		

Figure 1. Example of a horizontal HRSG [2, 3] in energy transfer processes.
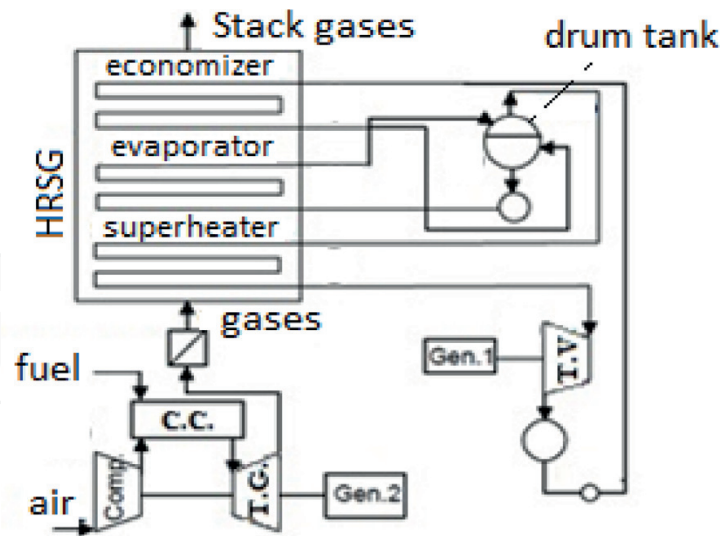
Figure 2. Modular strategy in modeling a steam generation system [4].

equipment life. Examples of modeling efforts are discussed with basic configuration of boiler furnaces and HRSG that includes economizer, evaporator, and super-heater modules. Moreover, the methodology proposes a modular approach strategy such as the one depicted in **Figure 2**.

The technical literature shows models that permit the evaluation of transient processes in boilers and vapor generators. Those models are based in first principle thermo-hydraulic equations and some of the most important ones are discussed as follows. Mansour [4] studies the prediction of transient behaviors of combined cycle gas turbine (CCGT) plants and describes mathematical models of the dynamic behavior of the main components in the combined cycle process. His study describes the heat transfer equations of superheater, evaporator, and economizer that allow him to develop a numerical model and simulation system. His results are validated with field measurements from a power unit in Egypt. Dumont [5] describes models for HRSG in boilers "once-through" without drums. The economizer, superheater, and evaporator models are lumped in one complex main super-model, which is complex and difficult to differentiate individual component output variables. Dieck-Assad [6, 7] presents the development of a boiler model departing from first principle equations. This chapter adopts methodologies used in [6, 7] to model drum-evaporator systems considering specific modular control volumes and state variables that describe the dynamics of the energy transfer process from flue gases to the working fluid.

2. Modeling methodology

The first principle equations used to develop a steam generation process model require simplifications and assumptions that limit the scope and application for which the model is

created. Also, if control system optimization is desired, a performance index is defined and the accuracy predictions should be within tolerances defined by the amount of improvements expected by the original application goals.

For instance, a HRSG consists of a tandem of heat exchangers such that their mathematical modeling uses the governing equations from heat transfer, fluid dynamics thermal properties of tube materials, and thermal properties of water. The heat exchange physical phenomena involve nonlinear models that produce complex equation systems to represent a typical heat exchange process. In predicting the steady state and transient operation, the governing equations require a set of assumptions and considerations such as:

- The hot (flue) gases inertia is neglected.

- Heat loss around a heat exchanger control volume is not considered.

- The combustion gases flow has a uniform homogeneous distribution across the tube interchange area.

- The combustion gases coming from the turbine are considered to behave ideal at a pressure of 1 atm.

- The tubes in a distributed arrangement are identical, in other words, the water-vapor mass flow rate divides among the number of tubes leaving the header and the quantity of flue gases between tubes is the same.

- The following considerations are made at each module: at the economizer, the water flowing is at saturated liquid conditions, in the evaporator, we assume two phases at saturated conditions, and in the superheater, only superheated steam is considered except for the control volume of the attemperator system.

2.1. Heat exchangers

The gas flow coming from the turbine has also a pressure loss through the heat exchange process, however, this work focus on the internal behavior of the heat exchange fluid, and therefore, the velocity, pressure, and composition of flue gases are the same as the entering conditions to the first module. The superheater and economizer are considered as large heat exchangers where the flue gas follows trajectories similar to the ones shown in **Figure 3**. The water flows through a series of tube banks, which are aligned in normal directions to hot gases flow coming from the turbine. The tube banks are parallel among them and they are tied together with U tube connections as shown in **Figure 3**.

Figure 4 shows the traversal view of the tube bank heat exchange structure. This traversal view is composed by small control volumes represented in **Figure 5**. The energy equations in the x-y plane for gas, water, and metal have been reported in [4] and they are shown as follows.
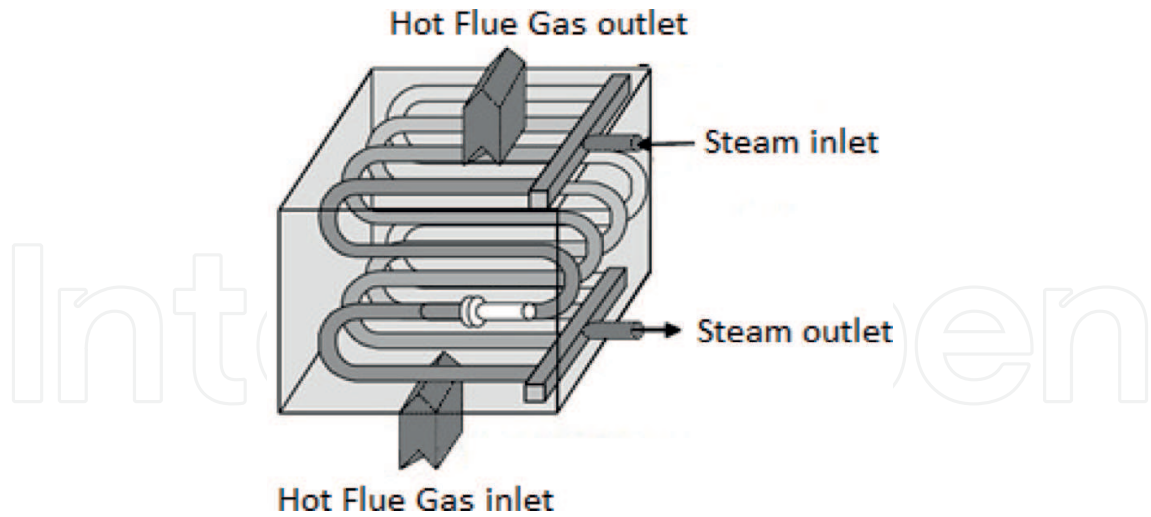
Figure 3. Multistage crossing flow heat exchange structure for economizer and superheater [4].
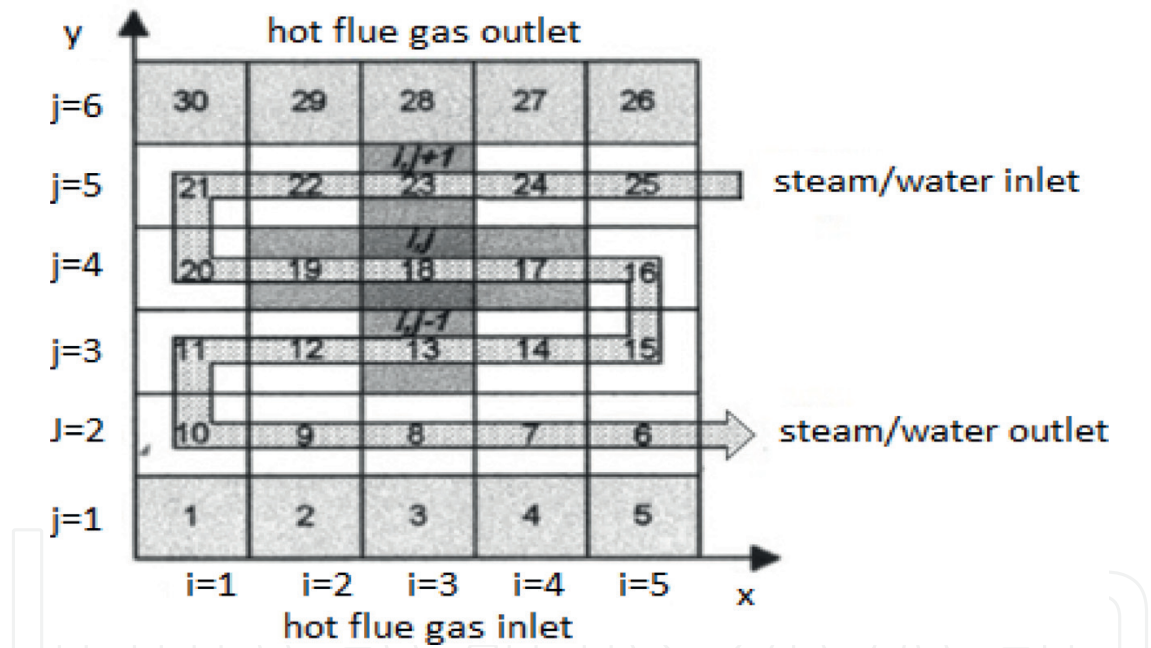

Figure 4. Traversal view representation of a heat exchange surface control volumes at modules of typical heat transfer tube surface (Plane x-y) [4].

For gas:

$$\frac{\partial T_g}{\partial t} + \gamma u_g \frac{\partial T_g}{\partial y} = -\frac{\dot{Q}_{gm}}{\rho_g V_g c_v} + \frac{\lambda_g}{\rho_g c_v}\left(\frac{\partial^2 T_g}{\partial y^2}\right) \tag{1}$$
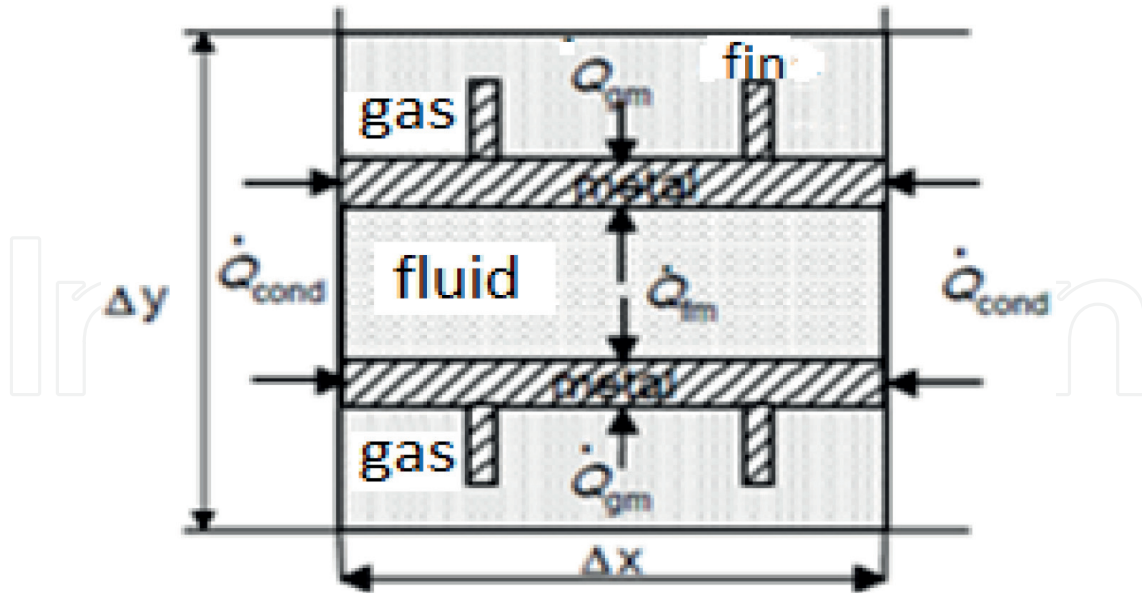
Figure 5. Control volume representation numerical meshes modules in typical heat transfer surfaces [4].

For water:

$$\frac{\partial T_f}{\partial t} + u_f \frac{\partial T_f}{\partial x} = -\frac{\dot{Q}_{fm}}{\rho_f V_f c_p} + \frac{\lambda_f}{\rho_f c_p}\left(\frac{\partial^2 T_f}{\partial x^2}\right) \tag{2}$$

For metal:

$$\frac{\partial T_m}{\partial t} = \frac{\dot{Q}_{gm} + \dot{Q}_{fm}}{\rho_m V_m c_m} + \frac{\lambda_m}{\rho_m c_m}\left(\frac{\partial^2 T_m}{\partial x^2}\right) \tag{3}$$

Every tube element is treated as a system group due to the fact that the Biot number (the ratio between the conduction heat transfer to convection heat transfer over the body surface) is less than 0.1. The rate of heat transfer from the hot flue gases to the metal tube is:

$$\dot{Q}_{gm} = A_o h_{gm}\left(T_g - T_m\right) \tag{4}$$

The rate of heat transfer from the tube walls to the internal fluid (water/steam) is determined as follows:

$$\dot{Q}_{fm} = A_i h_{fm}\left(T_f - T_m\right) \tag{5}$$

Eqs. (1) and (3) describe the heat transfer mechanism between the tube banks for the heat exchanger and have the characteristic of a parabolic partial differential equation. In order to discretize the equations, the back in time implicit Euler's center space (BTCS) method was selected. This method is very stable both in time and space, and the step sizes in time and space have no restrictions to assure a good solution [5]. This method approximates the partial differential equation with finite differences between points as illustrated in **Figure 6**, where "t" is time step and "i" is the space step.
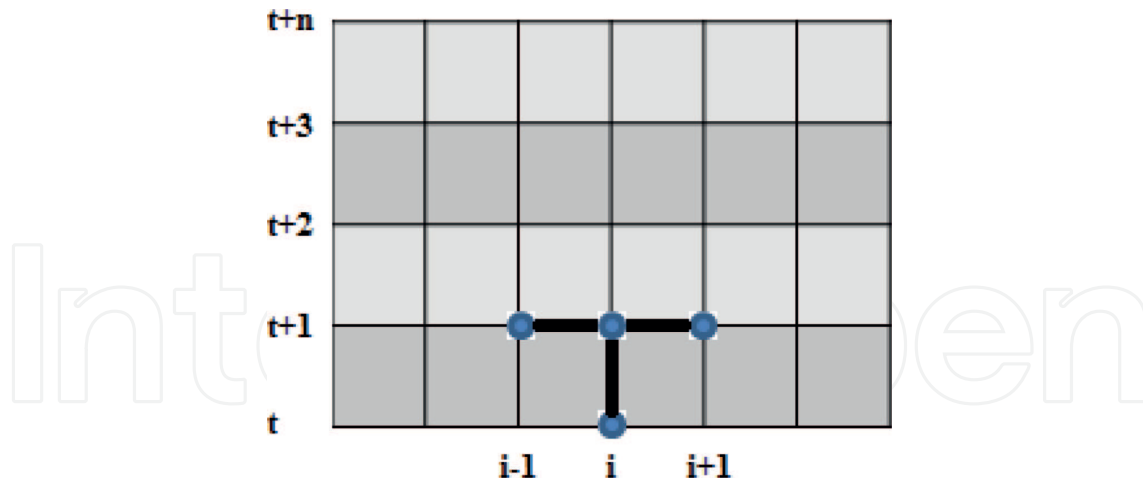
Figure 6. Scheme for the BTCS implicit method [5].

This way, an approximation to the partial differential equation is reached by finite differences, where each partial term of Eqs. (1)–(3) is represented by:

$$\frac{\partial \theta}{\partial \varphi} = \frac{\theta_i^{t+1} - \theta_i^t}{\Delta \theta} \frac{\partial \theta}{\partial \varphi} = \frac{\theta_i^{t+1} - \theta_i^t}{\Delta \theta} \tag{6}$$

$$\frac{\partial^2 \theta}{\partial \varphi^2} = \frac{\theta_{i-1}^{t+1} - 2\theta_i^{t+1} + \theta_{i+1}^{t+1} \partial^2 \theta}{\Delta \theta^2 \partial \varphi^2} = \frac{\theta_{i-1}^{t+1} - 2\theta_i^{t+1} + \theta_{i+1}^{t+1}}{\Delta \theta^2} \tag{7}$$

where θ represents any of the properties and ϕ any of the parameters.

Using the tube representation of **Figure 4** and establishing the numerical mesh from **Figure 5**, the following algebraic equations describe the heat transfer at the tube Banks:

• For flue gas

$$T_{g,i,j}^t = -bT_{g,i,j-1}^{t+1} + a_p T_{g,i,j}^{t+1} - aT_{g,i,j+1}^{t+1} - sT_{m,i,j}^{t+1} \tag{8}$$

where,

$$a = \frac{\lambda_g \Delta t \Delta x}{\rho_g c_v V_g} \qquad b = \frac{\lambda_g \Delta t \Delta x}{\rho_g c_v V_e} + \frac{\gamma \dot{m}_g \Delta t}{\rho_g V_e N_x N_r}$$

$$s = \frac{A_o h_{gm} \Delta t}{\rho_g V_g c_v} \qquad a_p = 1 + a + b + s \qquad s = \frac{A_o h_{gm} \Delta t}{\rho_g V_g c_v} \qquad a_p = 1 + a + b + s \tag{9}$$

• For metal

$$T_{m,i,j}^t = -aT_{m,i-1,j}^{t+1} + a_p T_{m,i,j}^{t+1} - aT_{m,i+1,j}^{t+1} - bT_{g,i,j}^{t+1} - sT_{f,i,j}^{t+1}$$
$$T_{m,i,j}^t = -aT_{m,i-1,j}^{t+1} + a_p T_{m,i,j}^{t+1} - aT_{m,i+1,j}^{t+1} - bT_{g,i,j}^{t+1} - sT_{f,i,j}^{t+1} \tag{10}$$

where,

$$a = \frac{\lambda_m \Delta t \Delta y}{\rho_m c_m V_m} \quad b = \frac{A_o h_{gm} \Delta t}{\rho_m V_m c_m}$$

$$s = \frac{A_i h_{fm} \Delta t}{\rho_m V_m c_m} \quad a_p = 1 + 2a + b + s \, s = \frac{A_i h_{fm} \Delta t}{\rho_m V_m c_m} \quad a_p = 1 + 2a + b + s \tag{11}$$

- Water/vapor

$$T_{f,i,j}^t = -b T_{f,i-1,j}^{t+1} + a_p T_{f,i,j}^{t+1} - a T_{f,i+1,j}^{t+1} - s T_{m,i,j}^{t+1}$$
$$T_{f,i,j}^t = -b T_{f,i-1,j}^{t+1} + a_p T_{f,i,j}^{t+1} - a T_{f,i+1,j}^{t+1} - s T_{m,i,j}^{t+1} \tag{12}$$

where,

$$a = \frac{\lambda_f \Delta t D_i}{\rho_f c_p V_f} \quad b = \frac{\lambda_f \Delta t D_i}{\rho_f c_p V_f} + \frac{\dot{m}_f \Delta t}{\rho_f V_f N_t}$$

$$s = \frac{A_i h_{fm} \Delta t}{\rho_f V_f c_p} \quad a_p = 1 + a + b + s \tag{13}$$

Ordering the algebraic representation of those equations for each of the discretization points, we can obtain a tri-diagonal matrix, which is solved using a standard Gauss elimination algorithm [8]. Therefore, this procedure allows us to evaluate the temperature behavior of the tube bank at each time step, in other words, its transient behavior.

The heat transfer coefficient between the flue gas and the tube bank structure is obtained using the Zukauskas correlation [9] as follows:

$$h_{gm} = \frac{\lambda}{D_o} E * B * Re^C * Pr_g^D \, h_{gm} = \frac{\lambda}{D_o} E * B * Re^C * Pr_g^D \tag{14}$$

where the coefficients B, C, and D are calculated according to the Reynolds number as described in **Table 1**.

where the Reynolds number is evaluated under maximum velocity conditions between tubes:

$$V_{max} = \frac{Pt}{Pt - D_o} V \, V_{max} = \frac{Pt}{Pt - D_o} V \tag{15}$$

In the case of heat transfer between the tube walls and the water/vapor fluid, we can use the Dittus-Boelter correlation for convection heat transfer as follows:

$$h_{fm} = 0.023 \frac{\lambda}{D_i} Re^{4/5} Pr^n$$
$$h_{fm} = 0.023 \frac{\lambda}{D_i} Re^{4/5} Pr^n \tag{16}$$

where n = 0.4 when the tube is at higher temperature than the working fluid (cooling) and n = 0.33 when the tube is at lower temperature than the working fluid (heating).

Staggered arrangement

Reynolds	B	C	D			
10–500	1.04	0.4	0.36			
1000–200,000 (Pt/Pl < 2)	0.35(Pt/Pl)^0.2	0.5	0.36			
1000–200,000 (Pt/Pl > 2)	0.4	0.6	0.36			
>200,000	0.022	0.84	0.36			
Line arrangement						
Reynolds	B	C	D			
0.4–4	0.89	0.330	1/3			
4–40	0.911	0.385	1/3			
40–4000	0.683	0.466	1/3			
4000–40,000	0.193	0.618	1/3			
40,000–400,000	0.0266	0.805	1/3			
E Coefficient N_{beds}->	1	2	3	4	5	
Line	0.7	0.8	0.9	0.9	0.9	1.0
Staggered	0.64	0.8	0.8	0.9	0.9	1.0

Table 1. Coefficients for the Zukauskas correlation [9].

2.2. Thermodynamic properties

The thermo-physical properties of the working fluids and flue gases that participate in heat exchange processes change with respect to temperature and pressure. Therefore, the thermo-dynamics properties model describes the water/vapor and hot gases behavior at different temperatures. The International Association of Properties of Water and Vapor, IAPWS, [10] proposes equations distributed in regions of thermodynamic state as illustrated in the pressure (p) versus temperature (T) diagram shown in **Figure 7**.

The simulation model integrates routines for the water thermodynamic properties, which are based and published in IAPWS-IF97 [10], "Release on the IAPWS Industrial Formulation 1997 for the Thermodynamic Properties of Water and Steam". For the thermodynamic properties of turbine waste gases, one can use the polynomials published by Yaws [11], which describe the behavior of each component in terms of temperature.

The heat transfer capacity in the tube banks is determined by the thermal conductivity, specific heat and density, which depend upon the operating temperature of the material. The ASME in "2001 ASME Boiler and Pressure Bessel Code, Section II – Materials" [12] describes and classifies the materials, which have similar behavior due to their chemical composition and their thermodynamic properties are shown as a function of the working temperature [13–15].
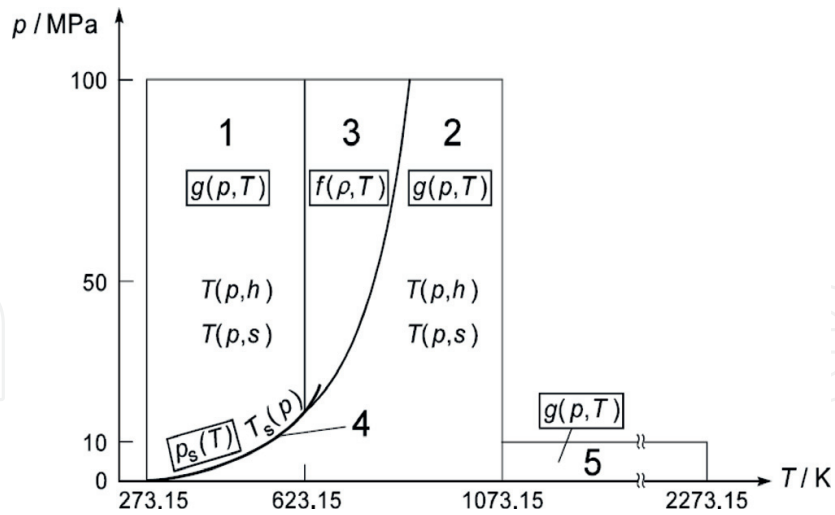
Figure 7. Distribution of thermodynamic property regions for modeling equations by IAPWS [9].

2.3. Drum-evaporator circuit

The evaporator consists of the thermal furnace system that includes drum tank, downcomer tubes, and riser tubes. The fluid circulation can be natural, assisted, or forced. **Figure 8** shows an evaporator thermal circuit that operates with natural water/steam circulation.

The numerical modeling of both control volumes, C.V.1 and C.V.2 shown in **Figure 8**, uses the proposed equations by Vega-Fonseca [16] and Dieck [6, 7, 17, 18], where the following assumptions are made:

- The mass flow rate that enters the downcomers (m_{dc}) equals to the mass flow rate received by the drum tank through the feedwater (m_{ec}).

- The water/steam flow circulation thru the risers and downcomers is constant.

- The liquid water at the drum tank is in saturation.

- The drum is a perfect cylinder.

- The feedwater flow to the drum coming from the economizer is at saturated liquid-water conditions.

The liquid level at the drum is obtained as follows:

$$\frac{dy}{dt} = \frac{\dot{m}_s\left[\frac{A_4}{A_2} - h_v\right] - \dot{m}_{ec}\left[\frac{A_4}{A_2} - h_{ec}\right] + \dot{Q}_r}{A_3 A_0 - \frac{A_1 A_4 A_0}{A_2}} \tag{17}$$

The drum pressure is obtained as follows:

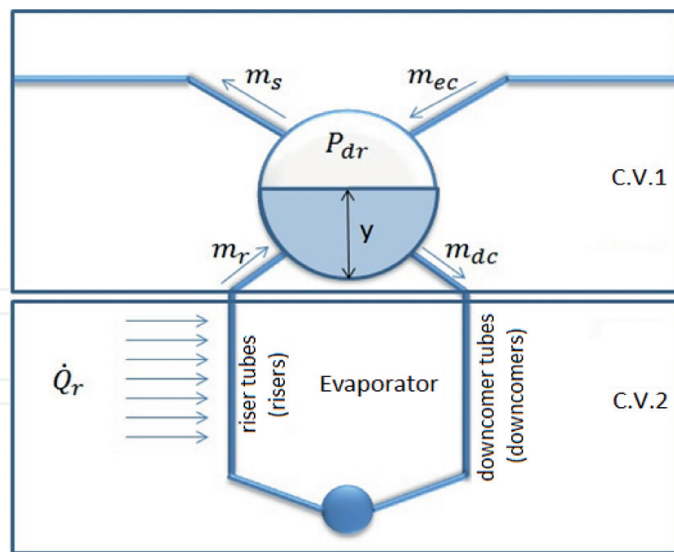**Figure 8.** Typical evaporation circuit.

$$\frac{dP}{dt} = \frac{\dot{m}_s\left[\frac{A_3}{A_1} - h_v\right] - \dot{m}_{ec}\left[\frac{A_3}{A_1} - h_{ec}\right] + \dot{Q}_r}{A_4 - \frac{A_3 A_2}{A_1}} \qquad (18)$$

The previous equations are complemented using the following Energy balance from the hot flue gases to the water steam as shown in **Figure 9**.
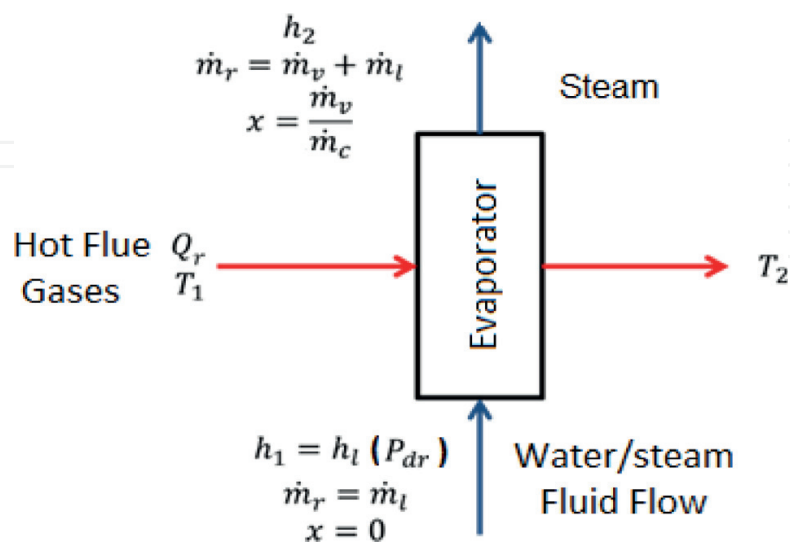

Figure 9. Energy balance at the evaporator.

$$x = \frac{\dot{m}_v}{\dot{m}_r} \qquad (19)$$

$$h_1 = h_l(P_{dr}) \qquad (20)$$

$$h_{lv} = h_v(P_{dr}) - h_l(P_{dr}) \qquad (21)$$

$$h_2 = x h_{lv} + h_1 \qquad (22)$$

$$\dot{Q}_r = \dot{m}_r(h_2 - h_1) \qquad (23)$$

To obtain the combustion gas temperature at the evaporator exit, the following equation can be used:

$$\dot{Q}_r = \dot{m}_g C_{p_g}(T_2 - T_1) \qquad (24)$$

Eqs. (15) and (16) describe the behavior of the drum-evaporator system in terms of the absorbed heat by the evaporator, the drum feedwater flow, and the vapor leaving the drum to the superheated system.

2.4. Shrink and swell model

In some steam generators, changes in temperature and pressure in the evaporator system produces an unbalance condition that generates a reverse effect in the drum level when increasing load conditions [7]. This phenomenon is called shrink and swell due to the vapor bubbles generated in the drum tank that generates the rise and drop of the drum level value. To model this effect, a first order transfer function term equation is proposed as follows:

$$\Delta h = \frac{K(W_{fe} - W_{sh})}{\frac{s}{\tau} + 1} \qquad (25)$$

where Δh is the drum level adjustment, τ is the bubble transit time to the drum liquid surface, W_{fe} is the feed-water flow, W_{sh} is the steam flow output to the high temperature exchangers such as the superheater, s is the complex frequency variable (s = jω), and K is a constant of the model in sec/Kg. This equation assumes that the bubbles are lumped into a volume section of the drum cylinder and Eq. (27) describes a first order behavior in transporting this volume to the very top of the liquid surface.

2.5. Control system model

The predicted performance of the HRSG expects the use of a three element drum level control system in the evaporator. This will allow a smooth control in the drum tank dynamic behavior. The configuration is based upon three process variables that are measured during the HRSG operation: output steam flow, drum liquid level and feedwater flow. The control system model assumes the use of PID controllers for the three element control system. Other possibilities exist and can be substituted by the PID algorithms.

The standard PID model is as follows:

$$G_c = k_p\left(E_t + \frac{1}{T_i}\int_0^t E_t dt + T_d \frac{dE_t}{dt}\right)$$
$$G_c = k_p\left(E_t + \frac{1}{T_i}\int_0^t E_t dt + T_d \frac{dE_t}{dt}\right) \quad (26)$$

where the discrete formulation is:

$$\Delta G_c = k_p\left[E_t - E_{t-\Delta t} + \frac{\Delta t}{2T_i}(E_t + E_{t-\Delta t}) + \frac{T_d}{\Delta t}(E_t - 2E_{t-\Delta t} + E_{t-2\Delta t})\right]$$
$$\Delta G_c = k_p\left[E_t - E_{t-\Delta t} + \frac{\Delta t}{2T_i}(E_t + E_{t-\Delta t}) + \frac{T_d}{\Delta t}(E_t - 2E_{t-\Delta t} + E_{t-2\Delta t})\right] \quad (27)$$

The first PID controller sets the demand for drum level that is compensated by the feedforward signal from the steam flow as shown in **Figure 10**. The compensated demand signal for drum level is compared to the measured feedwater flow signal to obtain the error signal that feeds the second PID controller that activates the feedwater valve actuator. Therefore, the use of three process signals: drum level, steam flow, and feedwater flow in the HRSG decreases the expansion and contraction behavior in the drum liquid due to sudden changes in steam load. Summarizing the drum level control includes the first PID controller, which determines the liquid level demands, and the second PID controller, which determines the feedwater to the drum tank.

The feedwater flow is controlled by modifying the cross sectional area of the valve, which is the percentage of opening. The following equations illustrate this controlling action.

$$E(AP_{wvy}) = y_r - y, \quad E(AP_{wv\dot{m}}) = \dot{m}_v - \dot{m}_w$$
$$\Delta AP_{wv} = \Delta G\left[E\left(AP_{wvy}\right)\right] + \Delta G[E(AP_{wv\dot{m}})]\Delta AP_{wv} = \Delta G\left[E\left(AP_{wvy}\right)\right] + \Delta G[E(AP_{wv\dot{m}})] \quad (28)$$

The steam flow, flowing out of the drum tank, is also modifying using the percentage of opening, however, this controller does not follow the liquid level signal, but the drum pressure of the HRSG. **Figure 11** shows how the drum pressure signal, that generates a demand signal, which is feedforwarded by the steam flow, obtains the demand for the vapor actuator valve. The following equations show the controlling action for the actuator of steam valve.
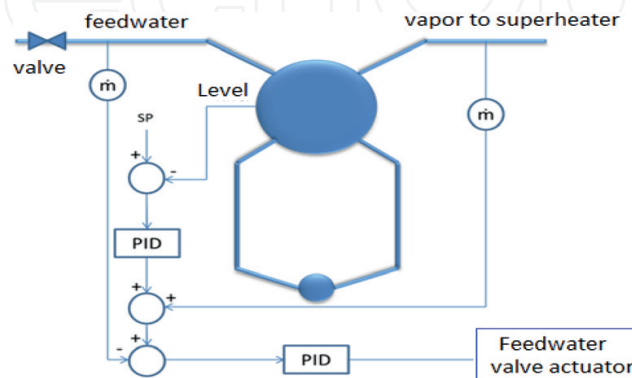
Figure 10. Drum level control system diagram.
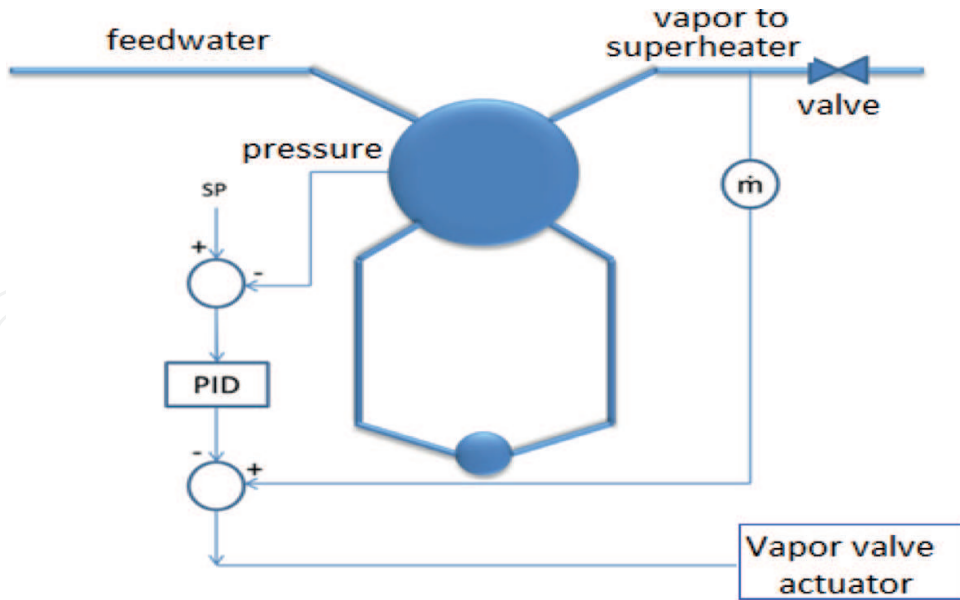
Figure 11. Drum pressure control system diagram.

$$E(AP_{sv}) = P_r - P$$
$$\Delta AP_{sv} = \Delta G\,[E(AP_{sv})]$$

(29)

Figure 12 shows the steam temperature control system that uses vapor attemperation to regulate the main steam thermal conditions going to the superheater system. The system compares the steam temperature at the superheater 2 outlet with the set point to generate the error. Then the PID controller generates the demand signal to open or close the spray valve, which brings water/vapor at lower temperature than the superheat leaving the drum.
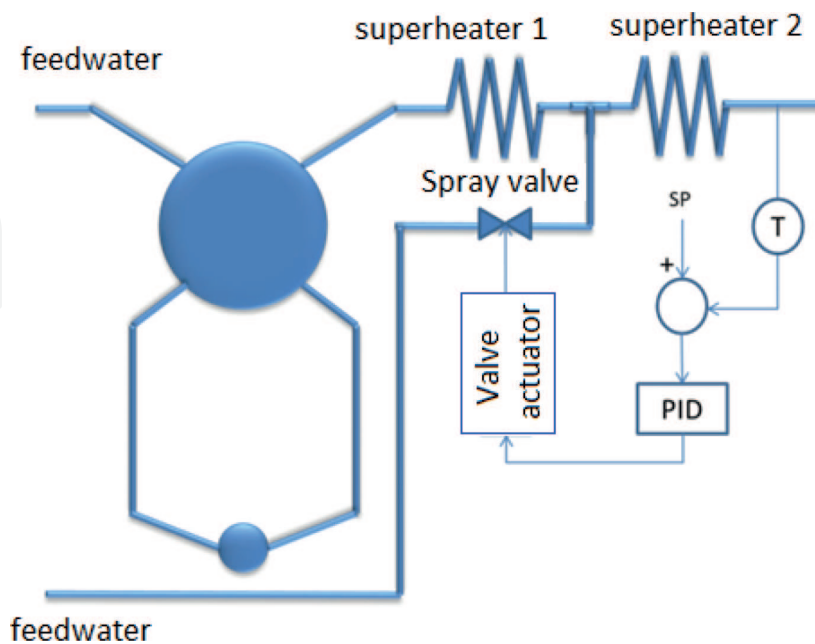
Figure 12. Steam temperature using feedwater attemperation. Control system diagram.

3. Simulator development

Once the equations have been derived, a computer simulation model is developed to initiate the test of the steam generation system predicted performance both, in steady state and dynamic conditions. One of the objectives is to validate a modular simulation feature that permits a fully integration of blocks when additional components are added to the system. The simulation tool would be useful to provide predicted performance behaviors for a wide variety of system configurations based in elementary modules such as preheaters, economizers, evaporators, superheaters, and reheaters. **Figure 13** describes the general operation of a typical computer simulation program where the main computing blocks and variables are described. Further details on the simulation blocks and programs can be found in Ref. [16].

3.1. Case study 1: Modeling and simulation of an industrial boiler

An industrial boiler was modeled and simulated having a traditional PID control strategy. The boiler under test was a $VU - 60$ Industrial system that produces 180,000 pounds of steam per hour [7]. The mathematical model of the plant was a scaled version model of the one obtained for a thermoelectric unit [6]. The model represented only the behavior of the drum-evaporator system having a combustion process with a simplified control system and a three element boiler feed-water controller. The simulations were performed using the SIMULINK® shell running under the MATLAB® platform.

The computational model obtained is compared with the measurements from the real boiler at steady state as well as during transient conditions. In steady state, four steam loads were studied and they are shown in **Tables 2–5**. In all cases, a small steady state error is observed
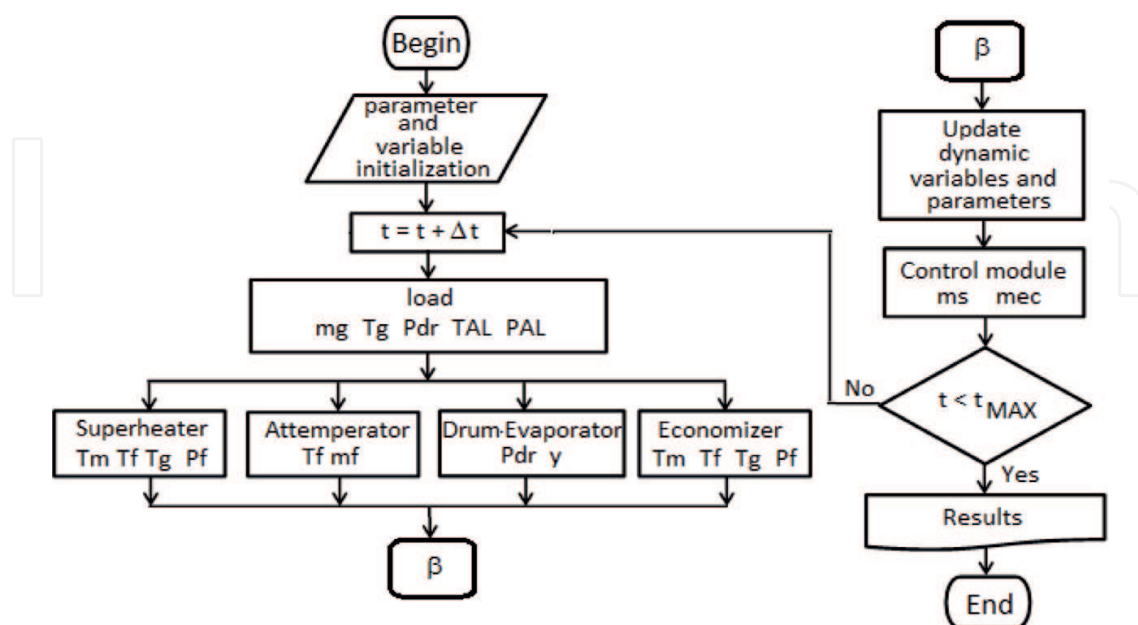

Figure 13. Computer simulation flow diagram.

@56e3 lb/h	Real	Simulated	Error
Steam flow (lb/h)	56.25e+3	56.25e+3	0.00%
Feed-water flow (lb/h)	56.25e+3	56.25e+3	0.00%
Gas flow (lb/h)	3.09e+3	3.18e+3	2.72%
Drum water level (in)	21.28e+0	21.28e+0	0.00%
Drum pressure (psia)	453.84e+0	453.84e+0	0.00%

Table 2. Measurement vs. simulation comparison for a load of 56×10^3 lb/h.

@65 e+3 lb/h	Real	Simulated	Error
Steam flow (lb/h)	65.73e+3	65.73e+3	0.00%
Feed-water flow (lb/h)	65.90e+3	65.73e+3	-0.26%
Gas flor (lb/h)	3.77e+3	3.71e+3	-1.55%
Drum water level (in)	25.93e+0	25.93e+0	0.00%
Drum pressure (psia)	445.44e+0	445.44e+0	0.00%

Table 3. Measurement vs. simulation comparison for a load of 65×10^3 lb/h.

@135e3 lb/h	Real	Simulated	Error
Steam flow (lb/h)	135.36e+3	135.36e+3	0.00%
Feed-water flow (lb/h)	141.88e+3	135.36e+3	-4.60%
Gas flow (lb/h)	8.04e+3	7.65e+3	-4.77%
Drum water level (in)	25.84e+0	25.84e+0	0.00%
Drum pressure (psia)	474.63e+0	474.63e+0	0.00%

Table 4. Measurement vs. simulation comparison for a load of 135×10^3 lb/h.

for the feed-water flow. This error might be produced by a purge located before the sensor position. This way the flow will always be higher in the simulation values.

The simulation of the transient behavior was performed using a load ramp of 1.9% per minute. The results for the critical variables are shown in **Figures 14** and **15**. The error in the feed-water flow is due to a non-minimal phase effect that was not replicated exactly in the model simulation.

@170e3 lb/h	Real	Simulated	Error
Steam flow (lb/h)	170.74E+3	170.74E+3	0.00%
Feed-water flow (lb/h)	175.40E+3	170.74E+3	-2.66%
Gas flow(lb/h)	9.87E+3	9.67E+3	-2.02%
Nivel Agua Domo(in)	25.73E+0	25.73E+0	0.00%
Drum pressure (psia)	502.17E+0	502.17E+0	0.00%

Table 5. Measurement vs. simulation comparison for a load of 170×10^3 lb/h.
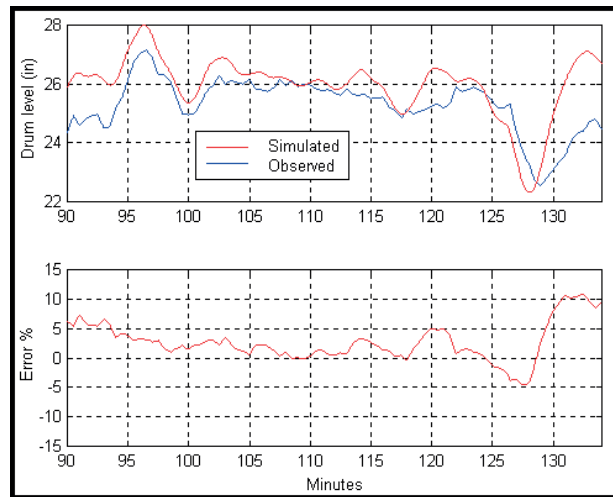
Figure 14. Drum level behavior and error comparing simulation and measurements.

3.2. Case study 2: Modeling and simulation of HRSG

This case shows a heat recovery steam generator (HRSG) operating at different ramping conditions and then settling a steady state operating. The modular simulation methodology permits a full integration of blocks when additional components are added to the system. The simulation tool provides predicted performance behaviors for a wide variety of HRSG configurations based in elementary modules such as preheaters, economizers, evaporators, superheaters, and reheaters. Further details on the simulation blocks and programs can be found in Ref. [16]. **Tables 6** and **7** shows the dimensions and geometries of the system.

The case in point describes the behavior of a load rejection from 100–75% in the turbine gas capacity, by making reductions in the amount of combustion gases as well as in their

Figure 15. Feedwater flow behavior and error comparing simulation and measurements.

Drum Tank		
Ld	Drum Lenght [m]	10.973
R	Drum Radius [m]	0.991
Y	Drum Liquid Level [m]	50%

Table 6. Geometric configuration of the drum tank.

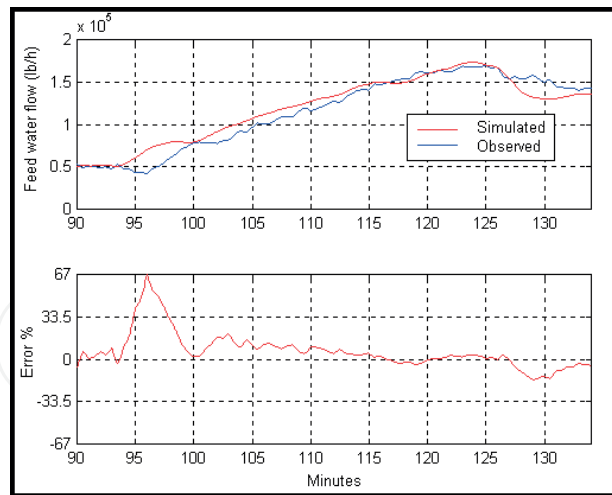| Geometry		SCAP1	SCAP2	SCAP3	ECAP1	ECAP2
Pl	Longitudinal step [m]	0.117475	0.117475	0.117475	0.092075	0.092075
Pt	Transversal step [m]	0.088011	0.088011	0.088011	0.088011	0.088011
OD	External diameter [m]	0.0381	0.0381	0.0381	0.0381	0.0381
THI	Tube thikness [m]	0.004191	0.003429	0.002667	0.002667	0.002667
Nt	Number of tubes per bed	64	64	64	64	64
Rfo	External waste factor [m^2-K/W]	0.000172	0.000172	0.000172	0.000172	0.000172
Lx	Tube lenght in X {m]	14.249	14.249	14.249	14.249	14.249
NR	Number of tube beds	2	2	2	7	7
la	Fin lenght [m]	0.009525	0.015875	0.015875	0.015875	0.015875
ta	Fin thickness [m]	0.000991	0.000991	0.000991	0.000991	0.000991
na	Number of fins per meter	118.1	226.4	226.4	259.8	258.9
Ws	Fin width [m]	0.003988	0.003988	0.003988	0.003988	0.003988
Rug	Absolute internal tube roughness [m]	0.000045	0.000045	0.000045	0.000045	0.000045

Table 7. Geometric configuration of the heat exchanger elements in the HRSG system.

temperatures. **Table 8** shows the how the variables change in the 900 seconds test. The control system generates corrective actions in order to sustain the liquid level and drum fluid pressure at the predicted performance. **Table 9** compares the simulated experiment results with the

100 to 75% ramping	Difference between loads	Rate of change per second
✽T_g (gas temp, °C)	-60	-0.067
✽m_g (gas mass flow, Kg/s)	-13.29	-0.015
✽T_f (steam temp, °C)	-9.5	-0.011
✽P_f (steam pressure, Bars)	-25.03	-0.028
✽P_{dr} (drum steam pressure, Bars)	-24.13	-0.027

Table 8. Variations of temperature, mass flow and pressures for 100–75% ramp.

predicted performance for the superheater systems. **Table 10** compares the simulated experiment results with the predicted performance for the evaporator and economizer systems.

Table 9 shows a 1.56% difference between the simulated steam flow at superheater 1 from the steady state predicted performance at 100% load. This result is due to a slight overestimation of the steam temperature at superheater 3 that induces the control system to inject spray water to regulate the steam temperature according to the reference value. **Table 10** shows also an overestimation of feedwater temperature at economizer 2. This temperature difference is 3.3% higher than the predicted performance for the HRSG system. However, those differences are well within the desired specifications of similar computer simulation systems. At the 75% load

			100% Load			75% Load		
		SIM	PERFORMANCE	ERROR	SIM	PERFORMANCE	ERROR
Hot Flue Gas Flow [Kg/s]		1213485.00	1213485.00	0.00%	1083578.00	1083578.00	0.00%
SUPERHEATER AP 1		SIM	PERFORMANCE	ERROR	SIM	PERFORMANCE	ERROR
STEAM FLOW [Kg/s]		203931.43	200800.00	-1.56%	149449.00	149449.00	0.00%
INLET	GAS TEMP [°C]	622.20	622.20	0.00%	562.20	562.20	0.00%
	FLUID TEMP [°C]	459.40	458.90	-0.11%	466.59	458.30	-1.81%
	FLUID PRESSURE[bar	92.89	92.87	-0.02%	69.45	69.43	-0.03%
OUTLET	GAS TEMP [°C]	605.18	605.60	0.07%	552.56	552.20	-0.07%
	FLUID TEMP [°C]	501.74	503.30	0.31%	497.07	492.80	-0.87%
	FLUID PRESSURE[bar	89.74	89.91	0.19%	67.12	67.22	0.14%
SUPERHEATER AP 2		SIM	PERFORMANCE	ERROR	SIM	PERFORMANCE	ERROR
STEAM FLOW [Kg/s]		203931.43	200703.00	-1.61%	149449.00	149449.00	0.00%
INLET	GAS TEMP [°C]	605.18	605.07	-0.02%	552.56	552.20	-0.07%
	FLUID TEMP [°C]	362.63	371.10	2.28%	384.14	376.70	-1.97%
	FLUID PRESSURE[bar	94.92	94.46	-0.49%	71.02	70.67	-0.50%
OUTLET	GAS TEMP [°C]	560.45	569.40	1.57%	524.80	526.10	0.25%
	FLUID TEMP [°C]	459.40	459.40	0.00%	466.59	458.30	-1.81%
	FLUID PRESSURE[bar	92.89	93.56	0.72%	69.45	69.91	0.66%
SUPERHEATER AP 3		SIM	PERFORMANCE	ERROR	SIM	PERFORMANCE	ERROR
STEAM FLOW [Kg/s]		197303.00	197303.00	0.00%	149449.00	149449.00	0.00%
INLET	GAS TEMP [°C]	560.45	560.45	0.00%	524.80	526.10	0.25%
	FLUID TEMP [°C]	308.11	308.30	0.06%	287.72	288.30	0.20%
	FLUID PRESSURE[bar	96.13	95.77	-0.37%	71.98	71.71	-0.38%
OUTLET	GAS TEMP [°C]	509.63	509.63	0.00%	481.11	487.80	1.37%
	FLUID TEMP [°C]	389.58	382.80	-1.77%	384.13	376.70	-1.97%
	FLUID PRESSURE[bar	94.92	95.15	0.24%	71.02	71.22	0.28%

Components: Superheaters AP-1, AP-2 and AP-3

Table 9. Comparison between initial and final loads for a download change from 100–75%.

		100% Load			75% Load		
EVAPORATOR		SIM	PERFORMANCE	ERROR	SIM	PERFORMANCE	ERROR
STEAM FLOW [Kg/s]		197303.00	197303.00	0.00%	149449.00	149449.00	0.00%
INLET	GAS TEMP [°C]	509.63	524.40	2.82%	481.11	487.80	1.37%
	FLUID TEMP [°C]	308.11	300.60	-2.50%	287.72	286.10	-0.57%
	FLUID PRESSURE[bar	96.13	96.11	-0.02%	71.98	71.98	0.00%
OUTLET	GAS TEMP [°C]	325.49	328.30	0.86%	306.18	305.00	-0.39%
	FLUID TEMP [°C]	308.11	308.90	0.26%	287.72	288.90	0.41%
	FLUID PRESSURE[bar	96.13	96.11	-0.02%	71.98	71.98	0.00%
ECONOMIZER AP 1		SIM	PERFORMANCE	ERROR	SIM	PERFORMANCE	ERROR
STEAM FLOW [Kg/s]		197303.000	197303.000	0.00%	149449.000	149449.000	0.00%
INLET	GAS TEMP [°C]	323.99	323.90	-0.03%	301.18	300.00	-0.39%
	FLUID TEMP [°C]	267.95	259.40	-3.30%	258.74	259.40	0.25%
	FLUID PRESSURE[bar	97.28	96.94	-0.35%	72.55	72.46	-0.12%
OUTLET	GAS TEMP [°C]	292.89	292.20	-0.24%	282.95	275.00	-2.89%
	FLUID TEMP [°C]	307.85	300.60	-2.41%	288.08	286.10	-0.69%
	FLUID PRESSURE[bar	96.73	96.11	-0.65%	72.24	71.98	-0.36%
ECONOMIZER AP 2		SIM	PERFORMANCE	ERROR	SIM	PERFORMANCE	ERROR
STEAM FLOW [Kg/s]		197303.00	197303.00	0.00%	124501.00	124502.00	0.00%
INLET	GAS TEMP [°C]	292.89	292.20	-0.24%	282.95	275.00	-2.89%
	FLUID TEMP [°C]	185.60	185.60	0.00%	176.10	176.10	0.00%
	FLUID PRESSURE[bar	97.77	97.77	0.00%	72.74	72.74	0.00%
OUTLET	GAS TEMP [°C]	237.63	242.20	1.89%	244.58	235.00	-4.08%
	FLUID TEMP [°C]	267.95	259.40	-3.30%	258.74	259.40	0.25%
	FLUID PRESSURE[bar	97.28	96.94	-0.35%	72.55	72.46	-0.12%

Components: Evaporator, Economizer AP-1 and Economizer AP-

Table 10. Comparison between initial and final loads for a download change from 100 to 75%.

a hot flue gases temperature error of 4.07% above the predicted performance is obtained from the computer simulation.

4. Conclusions

This chapter presents a methodology of a modeling and simulation of the steam generation process conceived as a development tool that permits the evaluation of different operating conditions of Industrial Boiler and HRSG systems. The objective is to support critical engineering decisions with respect to design, fault evaluation, and integrated analysis. Also, the simulation system allows the development of simulation exercises about interest scenarios to determine important multivariable cause-effects in both, industrial boilers and HRSG systems, without exposing the equipment to harmful and costly operative tests.

Two case studies are shown with validation tables both, in steady state and dynamic conditions. Even though the mathematical models are simplified, the results provide enough precision to study very complex dynamical behavior of this multivariable thermal process. Results show a difference of less than 5% with respect to the manufacturer's predicted performances in critical values of drum pressure, steam flow, steam temperatures, and hot flue gases flow. The numerical stability of the simulation behaves well due to the robustness of the discretization methodology and numerical methods used in the simulation model. The simulation model generates accumulated discrepancies and errors between 2 and 5% in temperature errors for the heat exchanger models such as economizers and superheaters. The drum pressure follows

the main steam demand as expected and the hot flue gases have a slight overshoot when the ramp ends at full nominal load. The controller showed a good performance maintaining the drum liquid level steady during all simulation exercises. Finally, the modular approach used can be expanded to include different geometric configurations and operating conditions, as well as different tuning alternatives for the control system [19–22].

Glossary

A	area (m^2)
c_p	specific heat at constant pressure (J/kg K)
c_v	specific heat at constant volume (J/kg K)
D	diameter (m)
E	error as a function of time
G	transfer function
g	gravity (m/s^2)
HRSG	heat recovery steam generator
h	entalpy (J/kg) or heat transfer coefficient (W/m^{2}K)
k_p	proportional gain
L	length (m)
M	mass (kg)
$\dot{m}$	mass flow rate (kg/s)
N_R	number of tube beds (or levels)
N_T	number of tubes per bed
P	pressure (bar)
P_l	longitudinal step (m)
P_t	transversal step (m)
PM	molecular weight (kg/moles)
P_r	Prandtl number
$\dot{Q}$	heat transfer rate (W)
r	radius (m)
Re	Reynolds number
t	time (s)

T	temperature (K)
T_i	integral time constant (s)
T_d	derivative time constant (s)
u	specific internal energy (J/kg)
V	velocity (m/s) or volume (m^3)
v	specific volume (m^3/kg)
x	coordinate x or vapor quality
Y	volumetric fraction
y	coordinate y or level (m)
f_d	friction coefficient
ε	roughness (m)
ξ	flow resistance coefficient
Υ	specific heat ratio
η	efficiency
D	change
λ	thermal conductivity (W/m K)
ρ	density (kg/m^3)
m	dynamic viscosity (Pa s)

Abbreviations

EVAP	high pressure evaporator
ECAP	high pressure economizer
TEF	inlet fluid temperature
TSF	outlet fluid temperature
TEG	inlet gas temperature
TSG	outlet gas temperature
SCAP	high pressure superheater

Sub-indices

c	refers to compound
dc	refers to downcomers
dr	refers to drum tank

ec	refers to economizer
f	refers to internal fluid
fm	refers to the transfer from fluid to metal
g	refers to gas
gm	refers to the transfer from gas to metal
h	refers to hydraulics
I	refers to internal
ll	refers to liquid water
m	refers to metal
mix	refers to a mixture
o	refers to external
r	refers to riser tubes or refers to reference value
s	refers to superheater
v	refers to water vapor
wh	refers to water header
ws	refers to the main steam valve
wv	refers to the feed-water valve

Author details

Graciano Dieck-Assad*, José Luis Vega-Fonseca, Isaías Hernández-Ramírez and
Antonio Favela-Contreras

*Address all correspondence to: graciano.dieck.assad@itesm.mx

Mechatronics and Electrical Engineering Department, Tecnológico de Monterrey, Monterrey
Campus, Monterrey, México

References

[1] Tomei GL. Steam Its Generation and Use, 42nd ed. Charlotte, North Caroline, U.S.A.: The Babcock & Wilcox Company; 2015

[2] Starr F. Background to the Design of HRSG Systems and Implications for CCGT Plant Cycling. OMNI. 2003;**2**

[3]   Stultz SC, Kitto JB, editors. Steam, Its Generation and Use, "Combined Cycles, Waste Heat Recovery and Other Steam Systems". 40th ed. Barberton OH: Babcock and Wilcox Co.; 1992. 31.1–31.13

[4]   Mansour FM. Combined Cycle Dynamics. IMechE Proc. Instn. Mech. Engrs., Vol. 217 Part A: J. Power and Energy; 2003

[5]   Dumont M-N. Mathematical modelling and design of advanced once-through heat recovery steam generator. Computers and Chemical Engineering, Elsevier. 2004;**28**(651):660

[6]   Dieck-Assad G. Development of a state boiler model for process optimization. Simulation. 1990;**55**:201-213

[7]   Dieck-Assad G. Modeling and simulation of a fuzzy supervisory controller for an industrial boiler. Simulation. 2006;**82**:841-850

[8]   Nakamura S. Metodos numericos aplicados con software. Mexico: Pearson; 1992

[9]   Zukauskas A. Heat Transfer from Tubes in Cross Flow. New York: Wiley Interscience; 1987

[10] International Association for the Properties of Water and Steam. IAPWS Industrial Formulation 1997 for the Thermodynamic Properties of Water and Steam

[11] Yaws, C. Yaws' 2003. Handbook of Thermodynamic and Physical Properties of Chemical Compounds. s.l.: Knovel

[12] American Society of Mechanical Engineers. 2001 ASME Boiler and Pressure Vessel Code, Section II–Materials, Subpart 2

[13] Crane Co. Flow of fluids through valves, fittings and pipe. Technical paper No. 410; 2009

[14] Incropera F. Fundamentals of Heat and Mass Transfer. 6th ed. USA: Wiley; 2007

[15] Holman JP. Heat Transfer. 6th ed. USA: McGraw-Hill; 1986

[16] Vega-Fonseca JL. Development of a simulator to study transients in Heat Recovery Steam Generator HRSG processes. Master's Thesis. Tecnológico de Monterrey, Monterrey Campus, México; 2012

[17] Dieck-Assad G. Midium Scale Modeling and Controller Optimization of a Boiler Turbine System. Phd dissertation. University of Texas at Austin, Austin, Texas, USA; 1984

[18] Dieck Assad G. Controllability and Optimization of Main Steam Temperature in Boilers with Burner Tilting, IEEE Mexicon. Guadalajara, Jalisco, Mexico; 1992

[19] Rovira V. A model to predict the behavior at part load operation of once-through heat recovery steam generators working with water at supercritical pressure. Applied Thermal Engineering. 2010;**30**:1652-1658

[20] Lee K. Analysis of thermal stress evolution in the steam drum during start-up of a heat recovery steam generator. International Journal of Energy Research. 2000;**24**(137):149

[21] Astrom KJL. Drum boiler dynamics. Automatica. 2000;**36**:363-378

[22] ALSTOM Clean Combustion Technologies. A Reference Book on Steam Generation and Emission Controls. 5th ed; 2010